AGN X

ROMA, 10-13/09/2012

Radio and gamma-ray emission in Faint BL Lacs

E. Liuzzo, B. Boccardi, M. Giroletti, G. Giovannini, F. Massaro, M. Orienti, S. Tamburri, C. Casadio

INAF ira

ALMA MATER STUDIORUM UNIVERSITÀ DI BOLOGNA A.D. 1088

STANFORD UNIVERSITY

Osservatorio Astronomico di Brera INAF

INSTITUTO de ASTROFISICA de ANDALUCIA CSIC I·A·A

γ - sky

3EG Catalog

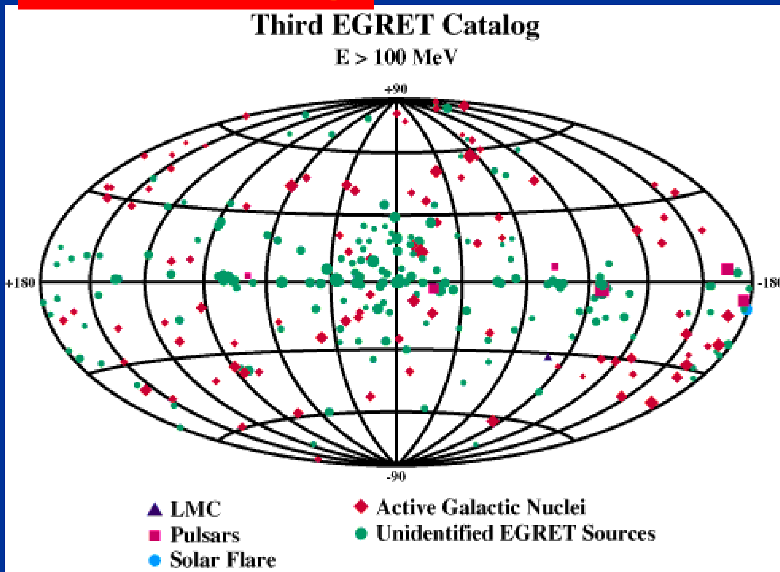

- **EGRET** (3EG, Hartman et al. 1999):

  Galactic plane emission + pulsars + blazars (#FSRQs > #BL Lacs)

2FGL Catalog

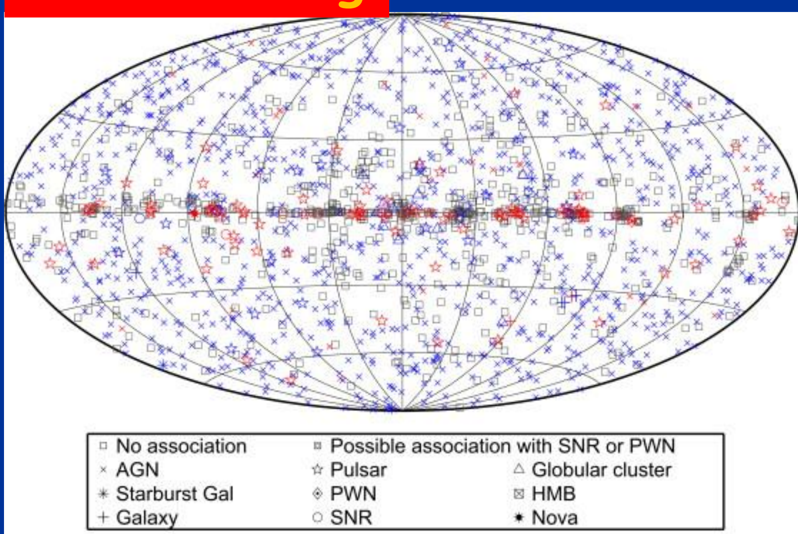

- ***Fermi*/LAT** (Ackermann et al. 2011):

  BL Lacs are the most common γ-ray emitters

Big open questions as...

origin of γ-ray flares
radio and γ correlation

The project

Giroletti et al. 2012, 2012AdSpR..49.1320G, Liuzzo et al. 2012 in prep.

Parsec scale properties of BL Lacs are poorly studied and VLBI survey are generally affected by small numbers, high flux density limits, incompleteness, etc

Goal:

Investigate the radio and gamma-ray connection in an homogeneous sample of **faint BL Lacs** using a multiwavelength approach.

The sample:

Sources selected from the Roma- BZCAT (M. Massaro et al. 2009) with :

- $z < 0.2$ → good linear resolution (1pc ~ 0,5 mas at z=0.1)
  → study also the week population of BL Lacs
- within the SDSS sky area → optical properties
  → kpc scale radio information (NVSS, FIRST)

Total #: 42 objects

The project

New observations:

VLBA data at 8 and 15 GHz for the whole sample
→ resolution of 1.6 mas at 8 GHz and 0.7 mas at 15 GHz
→ noise level of 0.2 mJy/beam

...an unexplored population:

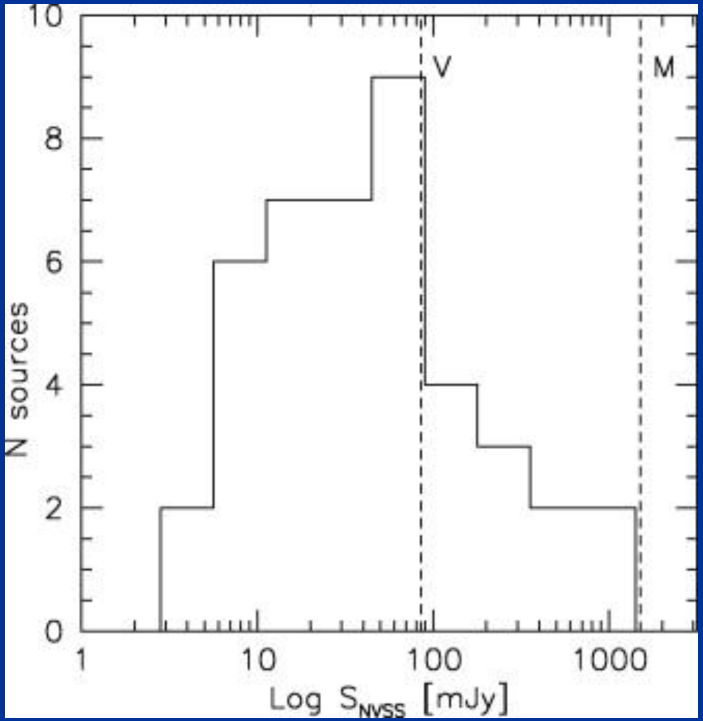

Distribution NVSS flux density for the sample sources

V : VIPS (S> 85 mJy, Helmboldt et al. 2007)
M: MOJAVE -1 (S> 1.5 mJy, Lister et al. 2009)
- - - : flux density limits extrapolated assuming α= 0

...with also information available on:

- X-ray emission (0.1-2.4 KeV) from the Roma BZCAT
- γ-ray emission: with 2 FGL

RESULTS - Radio

Absolute core position: some never studied sources were observed in phase referencing mode

Parsec scale morphologies:

- **Detection rate:** 67% at 8 GHz and 57% at 15 GHz
- **Point-like (p) sources:** 10/28 of detected sources at 8 GHz and and 17/24 at 15 GHz
- **One sided (1s) structures:** in 18 sources at 8 GHz and in 7 at 15 GHz (6 BL Lacs are 1s at both ν→ 5 are the most luminous at mas scales)

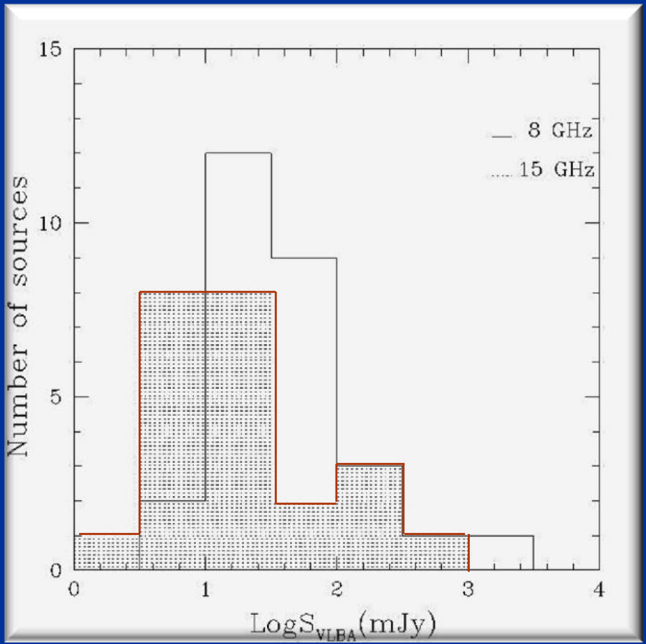

- **Total flux distributions:**
  ~ 70% of BL Lacs have fluxes in the range [10-40] mJy at 8 GHz and [4-20] mJy at 15 GHz

  →sample mostly composed by quite faint objects
  (some exceptions like J1217+3007, J1419+5423)

RESULTS - Radio

- **Spectral index distributions:**

$S \sim \nu^{-\alpha}$

Source compactness (SC):

CD= P(VLBA-8GHz) / P(NVSS)

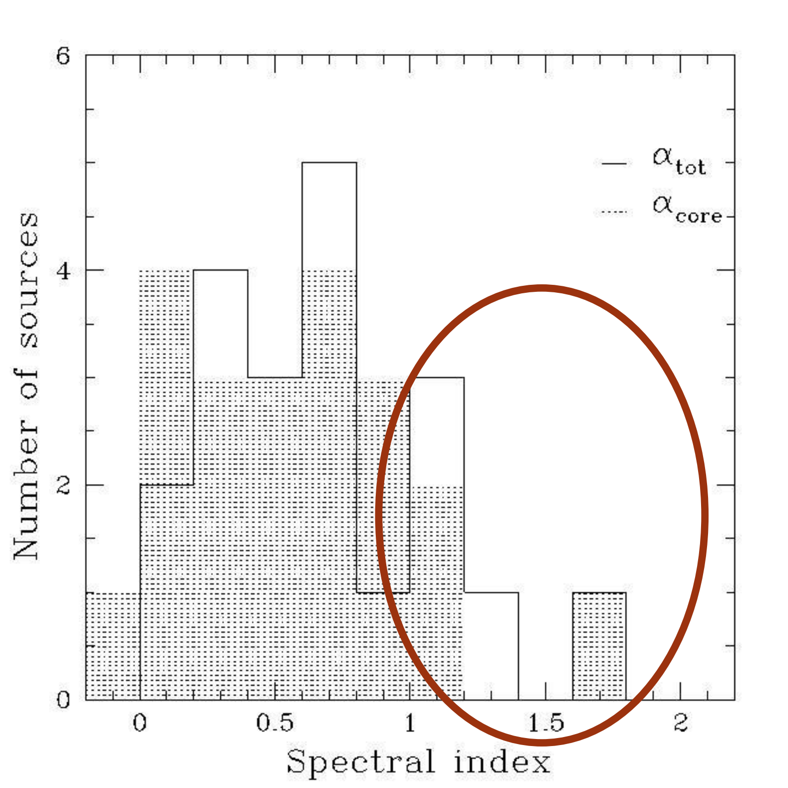

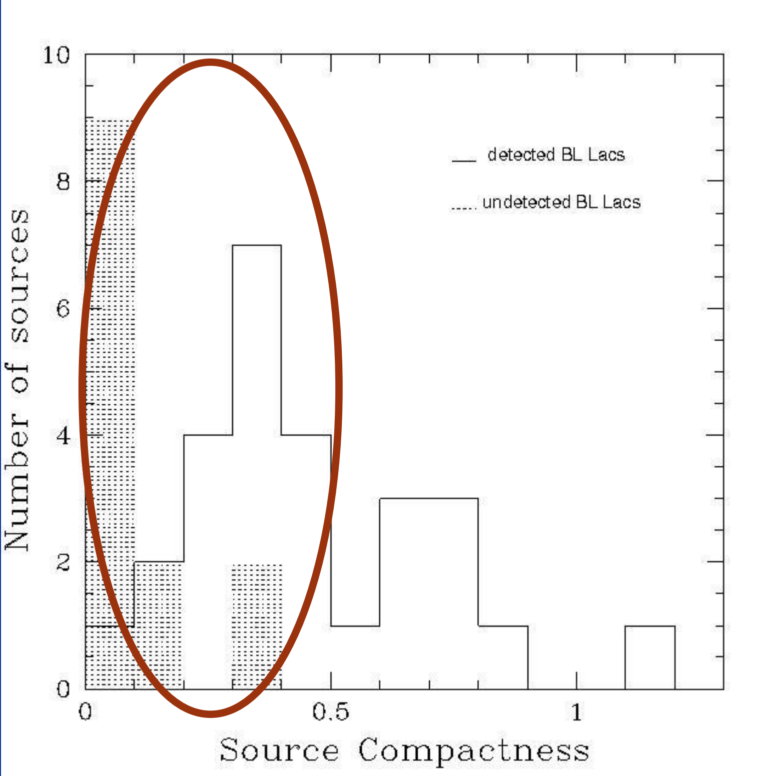

There is a considerable and unexpected number of sources with steep spectrum and low source compactness

RESULTS - Radio

Looking at pc and kpc scale radio properties, **4 groups** can be identified

- 3 Compact (C) sources: flat spectrum kpc and pc scale fluxes similar

- 19 Partially resolved (pR) sources: clearly visible VLBA core but some ≠ between kpc and pc scale flux densities, flat or moderately steep spectrum
  → sub-kpc structure?

- 15 Resolved (R) objects: SC $<$ 0.25 and/or steep spectrum
  → **new studied faint objects**

- 5 indeterminate (I) objects: undetected with also low kpc scale flux density
  → sensitivity is likely to be not enough
  → we are checking….

RESULTS - Gamma

Gamma- ray properties:

- **14/42 show high energy emission in 2LAC:** → **LAT BLACs**
  3 are C sources, 11 are pR . N:B no R BL Lacs are present

- Somes relations for the 2LAT BL Lacs....

S(Radio) vs S(Gamma)

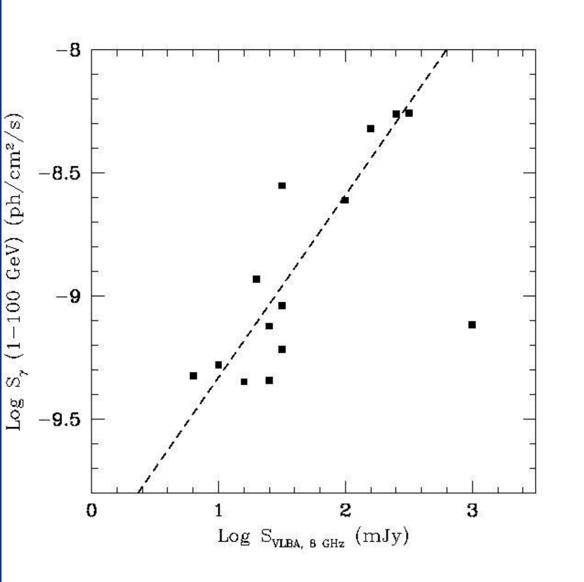

i=0.9 → Y= 0.74x-10.07

S(Radio) vs Photon index

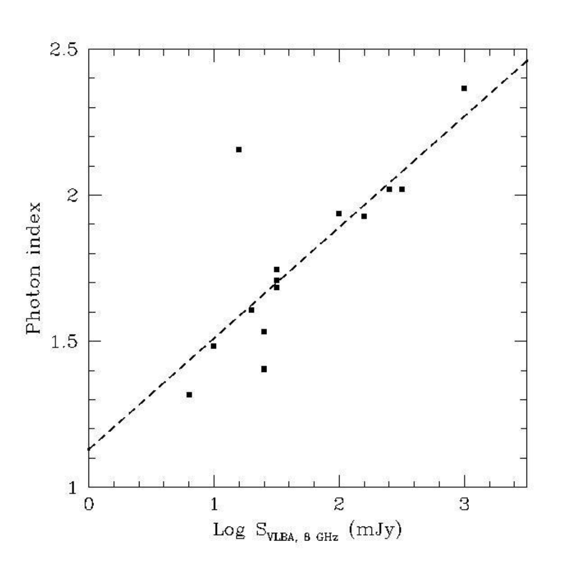

i=0.8 → Y= 0.38x+1.13

S(Gamma) vs S(X)

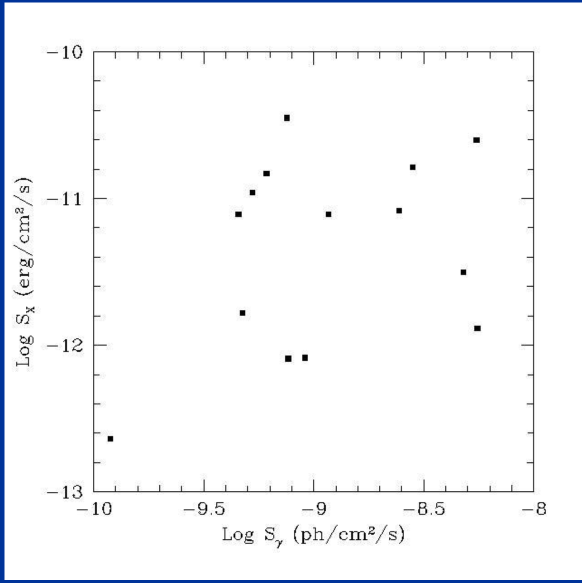

i=0.35 → no correlation

RESULTS – Peculiar cases

J1419+5423

6 cm VLBI maps

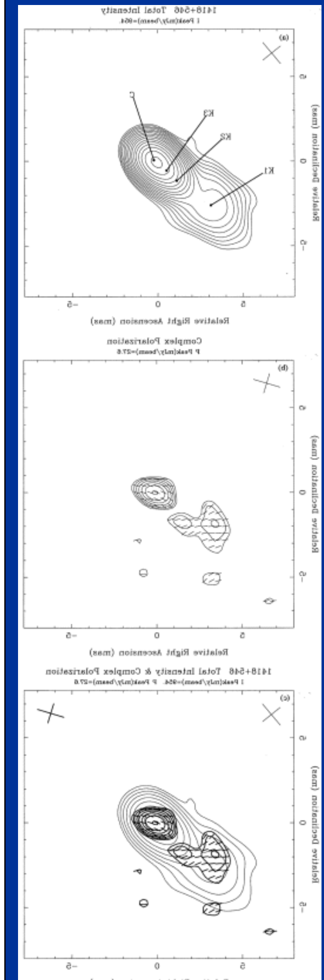

Gabuzda et al. 1999

- $LogP_{NVSS}$=25,68 (W/Hz) similar to $LogP_{VLBA-8GHz}$
- Point-like kpc structure
- SW VLBI jet (P.A.=130^0)
- Polarization in the core and in the jet with PPA aligned with the jet direction in the core, K3, and transverse in K2 (not clear for K1).
- Core: inverted spectrum at lower ν, and flat at higher ν
- Jet : spectral index from 0.2 (lower ν) to 0.5 (higher ν)
- B estimations

Spectral index distribution from 4.6-43 GHz

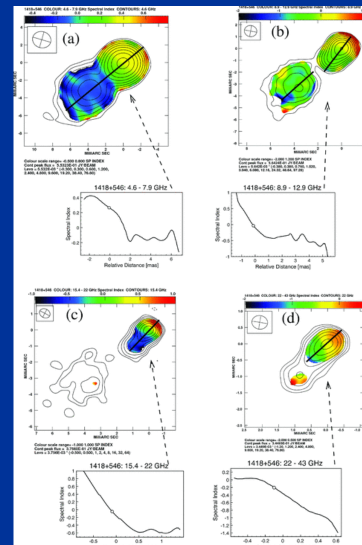

O'Sullivan et al. 2009

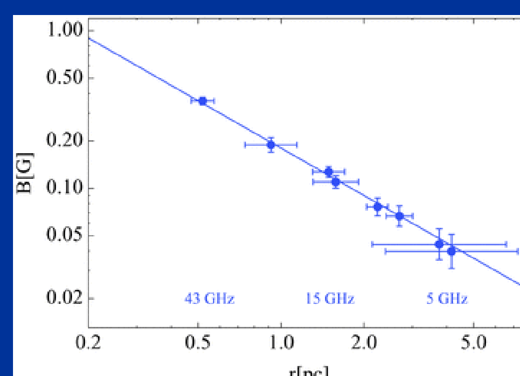

New VLBA observations

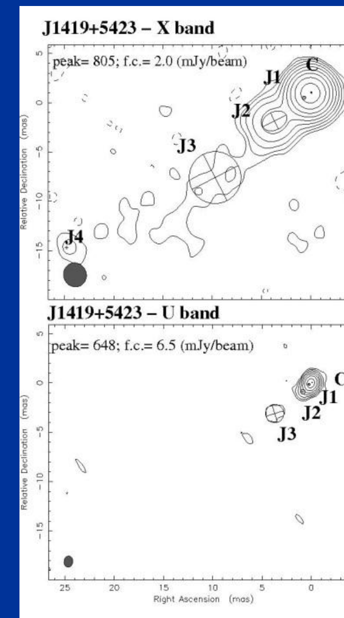

- Modelfitting→4 CC jet
  $S_{jet-8GHz}$=242,3 mJy
  $S_{jet-15GHz}$=385,1 mJy
  $\alpha_{tot,8-15GHz}$=0,3
  SC~1, βcoθ≥0,98

Other:

- Gamma-ray source

RESULTS – Peculiar cases

J1215+0732

Giroletti et al. 2006

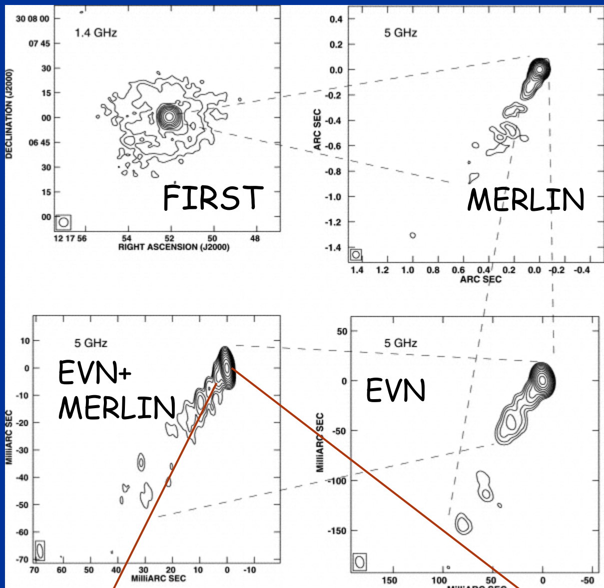

NEW!!

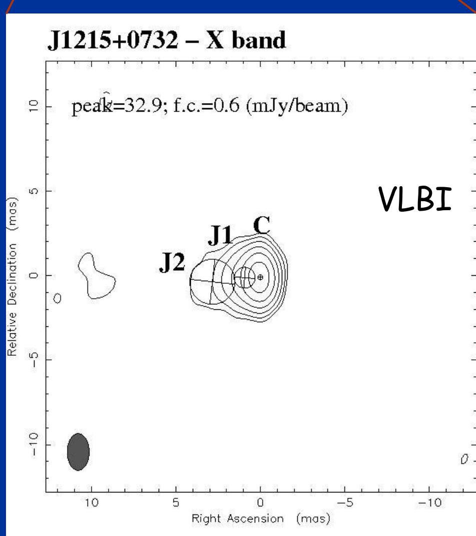

- $LogP_{NVSS}$=24,80 (W/Hz)
- $LogP_{8GHz-VLBA}$=24,31 (W/Hz)
- FIRST maps: core + symmetric halo of 50" diameter
- EVN scale: jet with P.A. = 140^0
- important effect of beaming (R>150)
- VLBA scale: 1s with 2 jet CC and total $S_{jet-8GHZ}$ =14,9 mJy but….
  Undetected at 15 GHz → ?!
- Low source compactness (SC = 0,33) → sub-kpc low surface brightness structure
- Other: No gamma-ray source

RESULTS - Radio/Gamma

Parsec scale morphologies:

- Among 1s sources at both ν (7/42), 5 are LAT BL Lacs which present the highest VLBA luminosities, as well source compactness.
- Among 1s sources at 8 GHz and unresolved at 15 GHz, 5 are LAT BL Lacs with no always the higher kpc flux densities (e.g. J1647+2909 is a no LAT BL Lac with S(NVSS)=395 mJy, while J1120+4212 is a LAT BL Lac with S(NVSS)=24 mJy)
- Unresolved structures at both frequencies are present indifferently in LAT and non LAT sources.

Name	8GHz struct	15GHz struct	S(8GHz) mJy	S(15GHz) mJy	S(NVSS) mJy	S(γ,1-100GeV) 10^{-10}ph/cm^2/s	Notes
J0809+5218	1s	P	97,8	73	183,8	24,49	pR
J0847+1133	P	-	9,0	<1,8	33,0	5,27	pR
J1053+4929	1s	P	30,7	13,0	65,5	9,15	pR
J1058+5628	1s	1s	164,4	141,1	229,5	47,88	C
J1120+4212	1s	P	20,3	18,1	23,5	11,69	C
J1136+6737	1s	p	31,1	16,2	45,2	6,10	pR
J1217+3007	1s	1s	262,3	217,4	587,8	54,92	pR
J1221+2813	P	p	337,2	226,2	739,0	55,39	pR
J1221+3010	1s	1s	29,5	23,4	72,0	28,12	pR
J1419+5423	1s	1s	959,5	819,7	818,2	7,66	C
J1428+4240	1s	P	22,5	10,8	57,5	7,54	pR
J1436+5639	P	p	6,5	6,2	20,7	4,74	pR
J1442+1200	1s	P	27,4	5,9	68,0	4,55	pR
J1534+3715	p	-	14,4	<1,2	21,0	4,49	pR

RESULTS - Radio/Gamma

Spectral index vs VLBA

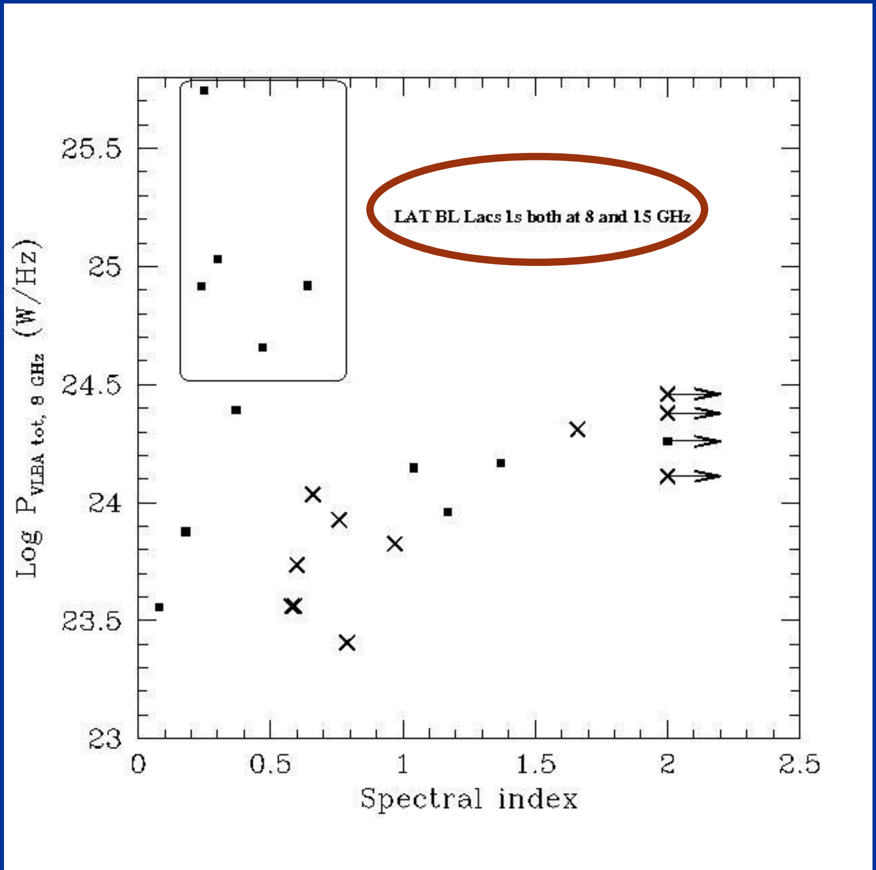

Source compactness vs VLBA

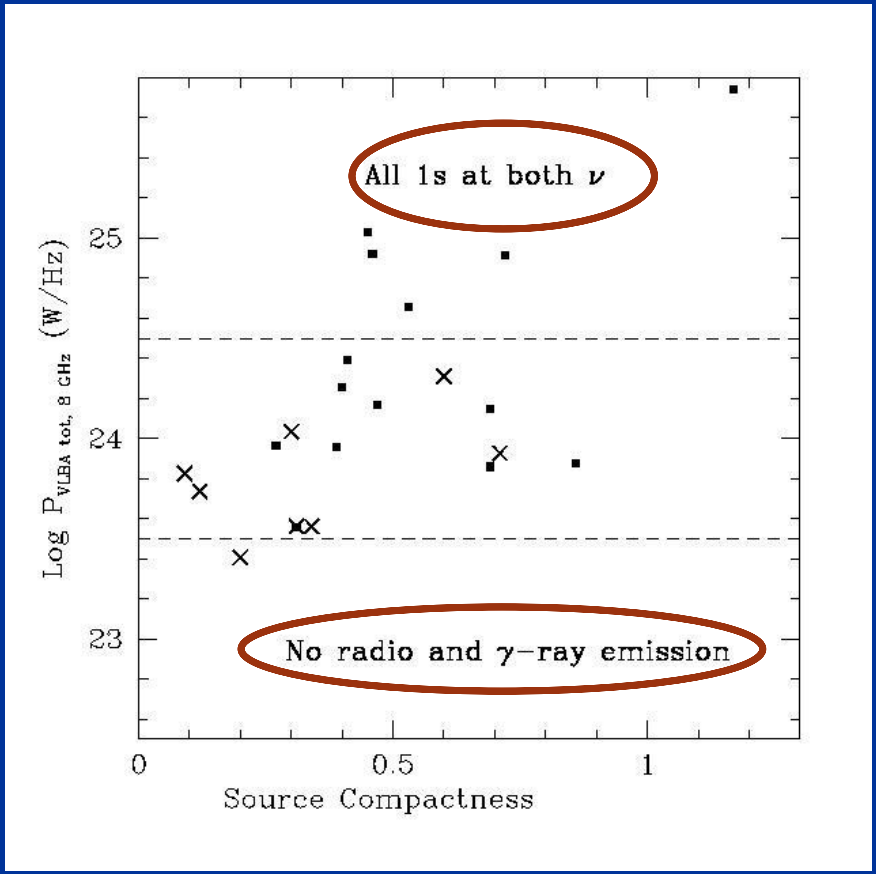

- LAT BL Lacs are the **most luminous** at parsec scale with 1s structure at both frequencies

- LAT BL Lacs with Log $P_{VLBA-8GHz}$ > 24.5 W/Hz have resolved morphology at both v
- **BL Lacs with Log $P_{VLBA-8GHz}$ < 23.5 W/Hz are not gamma-ray emitters**

RESULTS - Radio/Gamma

Spectral index vs Source Compactness

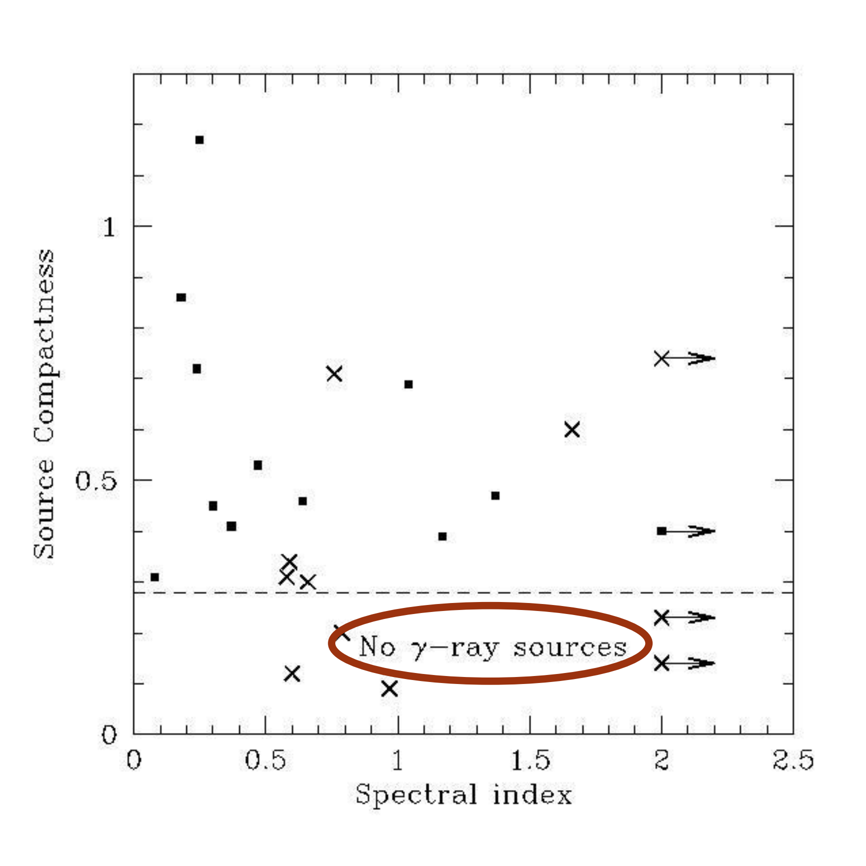

Gamma vs Source Compactness

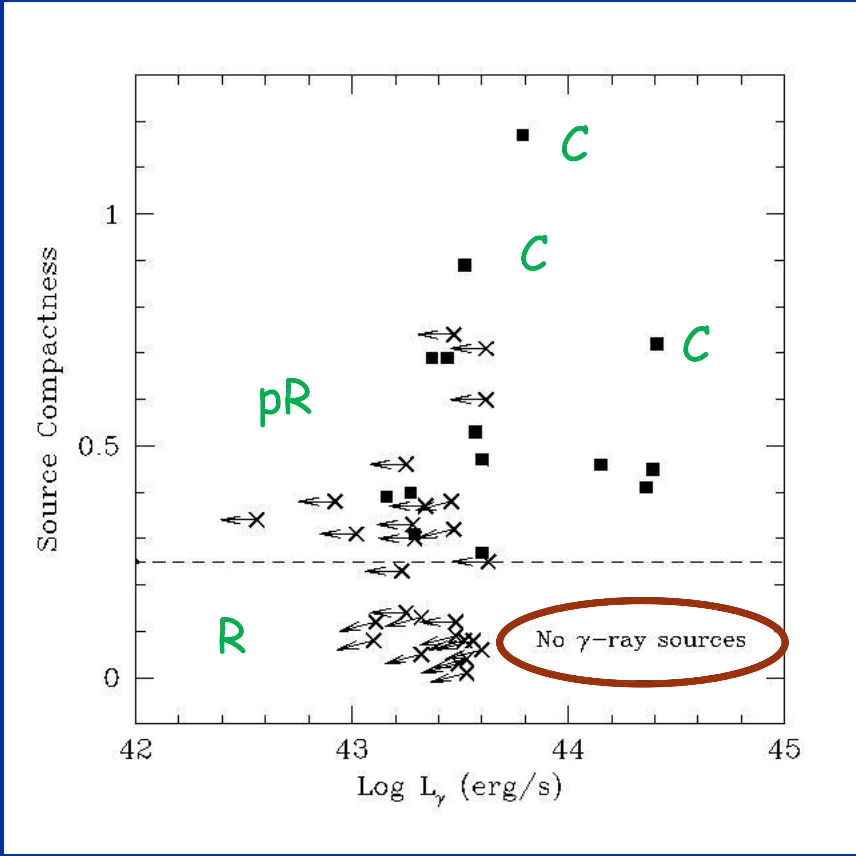

- Estimation of L_γ upper limits for non LAT BL Lacs
- The brightest LAT BL Lacs are not all C in radio band

Sources with SC<0.28 do not show gamma-ray emission

...In the WISE BLAZAR STRIP and in the WISE GAMMA-RAY STRIP

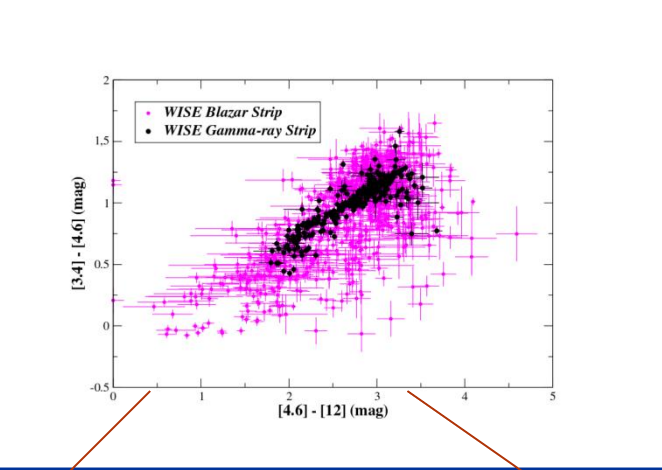

F. Massaro et al. 2012, (2012ApJ...750..138M)

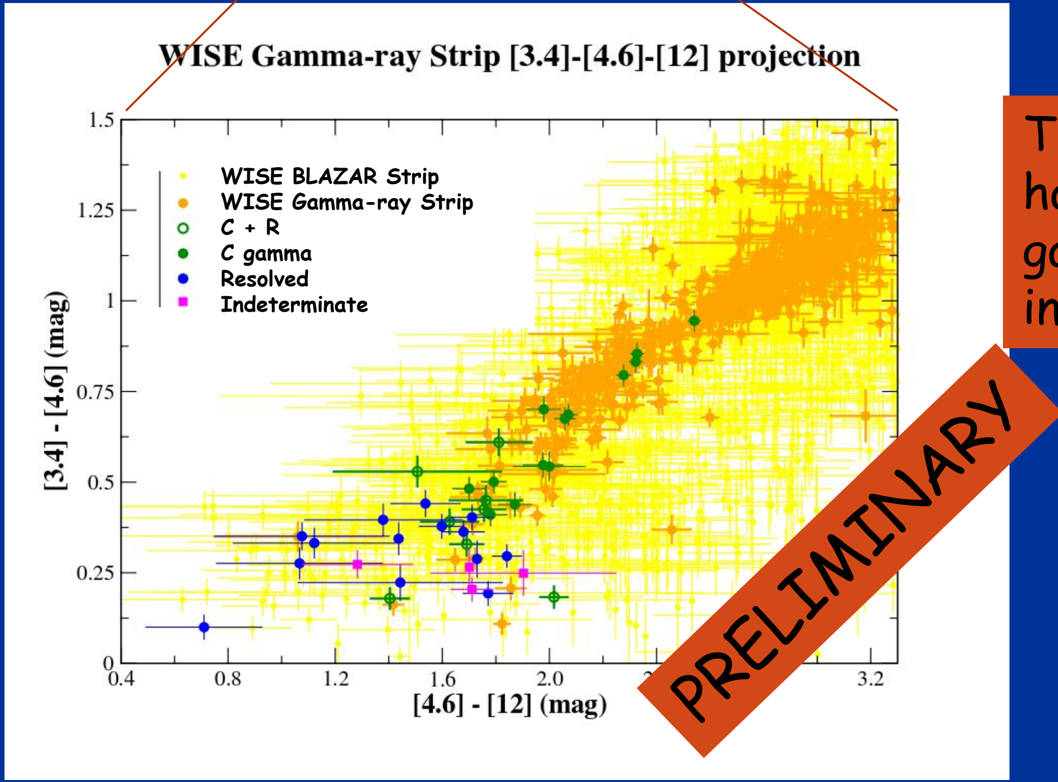

The 4 BL Lac groups have different radio, gamma and also infrared properties

CONCLUSIONS

- Fermi results show that BL Lacs are the most common gamma-ray emitters. Systematic parsec scale analysis on them were still missing.
- We selected an homogenous sample of nearby faint BL Lacs with no contraints on their radio and gamma-ray emission to study with a multiwavelength approach.
- New VLBA observations at 8 and 15 GHz are obtained and analysed for the whole sample.
- Based on spectral index and source compactness considerations, we distinguish 4 types of BL Lacs: C, pR, R, and I.
- We search for gamma-ray counterpart in the 2FGL Catalog: 14/42 BL Lacs show high energy emission.
- We investigated the radio and gamma correlation: SSC supported.
- Differences in the radio emission are observed among gamma-ray and non gamma-ray emitting objects.
- The source compactness seems to have the most important role in the high energy emission, but not only (see IR properties) → to check…
- Next steps will be the investigation of the nature of this radio /gamma-ray results (intrinsic differences in the power of the core? observational limits ? SED?)

THANK YOU

Table 5. Parsec scale morphologies and VLBA flux measurements for detected sources.

Name IAU	pc scale (8 GHz)	structure (15 GHz)	$S_{core,8.4GHz}$ mJy	$S_{tot,8.4GHz}$ mJy	$S_{core,15GHz}$ mJy	$S_{tot,15GHz}$ mJy	α_{core}	α_{tot}
J0754+3910	p	p	11.8±0.8	11.8±0.8	7.2±1	7.2±1	0.79±0.24	0.79±0.24
J0809+3455	1s	p	53.1±3.1	67.7±3.9	44.6±3.2	44.6±3.2	0.28±0.15	0.66±0.15
J0809+5218	1s	1s	74.3±4.4	97.8±5.7	58.0±4.2	73.0±5.2	0.39±0.15	0.47±0.15
J0847+1133	p	-	9.0±0.6	9.0±0.6	≤0.9	≤1.8	-	-
J0850+3455	p	-	12.7±0.8	12.7±0.8	≤0.9	≤1.8	-	-
J0903+4055	p	p	21.5±1.3	21.5±1.3	10.4±0.6	10.4±0.6	1.16±0.10	1.16±0.12
J0916+5238	p	p	22.2±1.7	22.2±1.7	7.8±1.1	7.8±1.1	1.66±0.26	1.66±0.26
J0930+4950	1s	1s	7.4±0.42	9.5±0.52	4.2±0.4	5.9±0.5	0.9±0.17	0.76±0.17
J1053+4929	1s	p	18.7±1.4	30.7±2.00	13.0±1.2	13.0±1.2	0.58±0.19	1.37±0.18
J1058+5628	1s	1s	106.1±6.2	164.4±9.6	100.8±7.1	141.7±10.0	0.08±0.15	0.24±0.15
J1120+4212	1s	p	18.7±1.1	20.3±1.2	18.1±1.4	18.1±1.4	0.05±0.16	0.18±0.16
J1136+6737	1s	p	15.4±0.9	31.1±1.8	16.2±1.6	16.2±1.6	-0.08±0.19	1.04±0.19
J1201-0007	p	p	8.00±0.6	8.0±0.6	5.5±0.9	5.5±0.9	0.60±0.30	0.60±0.30
J1215+0732	1s	-	30.7±1.80	45.6±2.7	≤0.6	≤2.1	-	-
J1217+3007	1s	1s	230.5±11.5	262.3±13.1	169.5±12.0	217.4±15.4	0.49±0.15	0.30±0.15
J1221+0821	p	p	15.8±0.9	15.8±0.9	8.6±2.1	8.6±2.1	0.97±0.42	0.97±0.42
J1221+2813	1s	1s	178.0±10.2	337.2±19.3	178.3±10.0	216.2±16.0	0.64±|0.15|	0.00±|0.15|
J1221+3010	p	p	29.5±1.9	29.5±1.9	23.4±1.8	23.4±1.8	0.37±0.17	0.37±0.17
J1231+6414	1s	p	31.5±1.9	43.5±2.5	1.6±0.5	1.6±0.5	4.74±0.54	5.25±0.54
J1253+0326	1s	p	35.1±2.1	36.6±2.1	25.2±1.8	25.2±1.8	0.55±0.15	0.59±0.15
J1419+5423	1s	1s	716.3±35.8	959.5±48.0	434.6±30.8	819.7±58.0	0.79±0.15	0.25±0.15
J1427+5409	1s	1s	12.0±0.8	13.7±0.9	7.8±0.6	9.5±0.7	0.69±0.17	0.58±0.17
J1428+4240	1s	p	20.7±1.22	22.5±1.3	10.8±1.1	10.8±1.1	1.03±0.20	1.17±0.20
J1436+5639	p	p	6.5±0.6	6.5±0.6	6.2±0.7	6.2±0.7	0.08±0.23	0.08±0.23
J1442+1200	1s	p	25.5±1.6	27.4±1.7	5.9±0.6	5.9±0.6	2.33±0.1	2.44±0.12
J1516+2918	1s	p	29.5±1.7	31.6±1.9	3.5±0.7	3.5±0.7	3.39±0.33	3.50±0.33
J1534+3715	p	-	14.4±0.8	14.4±0.8	≤0.6	≤1.2	-	-
J1647+2909	1s	p	48.5±2.8	56.4±3.3	7.0±1.2	7.0±1.2	3.08±0.30	3.32 ±0.30

In Col.s 1 and 2, "p" is for point-like morphology and "1s" for one-sided structure.

Table 6. Kiloparsec and parsec scale radio properties of the whole sample.

Name IAU	$\log P_{NVSS}$ W/Hz	$\log P_{core,8.4GHz}$ W/Hz	$\log P_{tot,8.4GHz}$ W/Hz	$\log P_{core,15GHz}$ W/Hz	$\log P_{tot,15GHz}$ W/Hz	$\beta\cos(\theta)$	SC	Notes
J0751+1730	23.93	≤22.72	≤23.02	≤22.72	≤23.02	-	≤0.06	R
J0751+2913	24.08	N.O.	N.O.	≤23.24	≤23.24	-	-	R
J0753+2921	23.41	≤22.99	≤22.99	≤22.89	≤22.89	-	≤0.38	U
J0754+3910	24.10	23.41	23.41	23.19	23.19	-	0.20	R
J0809+3455	24.56	23.93	24.03	23.85	23.85	≥0.92	0.30	pR
J0809+5218	24.93	24.54	24.66	24.43	24.53	≥0.86	0.53	pR
J0810+4911	23.53	≤22.58	≤22.58	≤22.88	≤ 22.88	-	≤0.12	R
J0847+1133	24.53	23.96	23.96	≤ 22.26	≤ 22.26	-	0.27	pR
J0850+3455	24.25	23.82	23.82	≤ 22.97	≤22.97	-	0.37	pR
J0903+4055	24.51	24.29	24.29	23.97	23.97	≥ 0.37	0.60	pR
J0916+5238	24.91	24.31	24.31	23.86	23.86	-	0.25	R
J0930+4950	24.27	23.82	23.93	23.57	23.72	≥0.56	0.71	pR
J1012+3932	24.15	≤23.04	≤23.04	≤23.19	≤ 23.19	-	≤0.08	R
J1022+5124	23.44	23.02	23.02	≤23.02	≤23.02	-	≤0.13	U
J1053+4929	24.50	23.95	24.18	23.80	23.80	≥0.60	0.47	pR
J1058+5628	25.06	24.73	24.92	24.70	24.85	≥0.27	0.72	C
J1120+4212	23.94	23.84	23.88	23.83	23.83	≥0.45	0.86	C
J1136+6737	24.31	23.84	24.15	23.87	23.87	≥0.89	0.69	pR
J1145-0340	24.11	≤22.63	≤22.63	≤23.10	≤23.10	-	≤0.03	R
J1156+4238	24.06	≤22.65	≤22.65	≤23.05	≤23.05	-	≤0.04	R
J1201-0007	24.68	23.74	23.74	23.57	23.57	-	0.12	R
J1201-0011	24.27	≤22.78	≤22.78	≤23.15	≤23.15	-	≤0.32	R
J1215+0732	24.80	24.14	24.31	≤22.98	≤22.98	≥0.92	0.33	pR
J1217+3007	25.38	24.98	25.03	24.64	24.95	≥0.93	0.45	pR
J1221+0821	24.88	23.83	23.83	23.56	23.56	-	0.09	R
J1221+2813	25.26	24.64	24.92	24.64	24.75	≥0.98	0.46	pR
J1221+3010	24.78	24.39	24.39	24.29	24.29	-	0.41	pR
J1231+6414	24.60	24.32	24.46	23.03	23.03	≥0.90	0.74	pR
J1253+0326	24.03	23.55	23.56	23.40	23.40	≥0.43	0.34	pR
J1257+2412	23.80	≤22.47	≤22.47	≤22.47	≤22.47	-	≤0.05	R
J1341+3959	24.80	≤22.83	≤22.83	≤22.83	≤22.83	-	≤0.01	R
J1419+5423	25.68	25.62	25.75	25.40	25.68	≥0.98	1.17	C
J1427+3908	23.68	≤ 22.61	≤22.61	≤23.31	≤ 23.31	-	≤0.09	U
J1427+5409	24.08	23.51	23.56	23.32	23.40	>0.48	0.31	pR
J1428+4240	24.37	23.92	23.96	23.64	23.64	≥0.33	0.39	pR
J1436+5639	24.06	23.56	23.56	23.54	23.54	-	0.31	pR
J1442+1200	24.65	24.23	24.26	23.59	23.59	≥0.52	0.40	pR
J1510+3335	23.36	≤22.27	≤22.27	≤22.27	≤22.27	-	≤0.08	U
J1516+2918	24.75	24.08	24.11	23.16	23.16	≥0.56	0.23	R
J1534+3715	24.02	23.86	23.86	≤22.78	≤22.78	-	0.69	pR
J1604+3345	23.75	≤22.68	≤22.68	≤22.68	≤22.68	-	≤0.08	U
J1647+2909	25.22	24.31	24.38	23.47	23.47	≥0.74	0.14	R

Col. 4: $\beta\cos\theta$ is derived from the jet/counterjet brigthness ratio. Where the counterjet is not detected, we took 3σ as its upper limit emission. Col. 5 SC indicates Source compactness. In Col. 6, R is for resolved sources, pR for partially resolved, C for compact ones, and U for Undeterminate objects (see details in Sect. 4.2). N.O. indicates source non observed with VLBA.

Table 7. Multiwavelength properties of the sample

Name	z	M_R	S_{NVSS} (mJy)	S_{FIRST} (mJy)	$S_{VLBA-8GHz}$ (mJy)	$S_{VLBA-15GHz}$ (mJy)	$F_{x(0.1-2.4keV)}$ (10^{-12} erg/cm^2/s)	$F_{\gamma(1-100GeV)}$ (10^{-10} ph/cm^2/s)
J0751+1730	0.185	18.2	9.72	10.96	<0.6	<1.2	1.78	-
J0751+2913	0.194	16.9	12.38	8.92	N.O.	<1.8	0.21	-
J0753+2921	0.161	15.7	3.96	4.49	<1.5	<1.2	1.29	-
J0754+3910	0.096	12.8	57.8	49.26	11.8	7.2	0.44	-
J0809+3455	0.083	12.6	227.43	169.12	67.7	44.6	4.07	-
J0809+5218	0.138	14.6	183.82	187.05	97.8	73.0	8.26	24.49
J0810+4911	0.115	13.5	10.76	10.91	<1.2	<2.4	0.2	-
J0847+1133	0.199	16.6	32.98	33.66	9.0	<1.8	11	5.27
J0850+3455	0.145	14.3	34.51	30.86	12.7	<1.8	0.65	-
J0903+4055	0.188	15.8	35.75	29.75	21.5	10.4	2	-
J0916+5238	0.190	15.0	88.41	108.93	22.2	7.8	3.83	-
J0930+4950	0.187	17.3	21.33	15.08	9.5	5.9	16.7	-
J1012+3932	0.171	16.0	19	20.11	<1.50	<2.1	0.65	-
J1022+5124	0.142	16.7	5.59	2.69	<2.1	<2.1	3.44	-
J1053+4929	0.140	13.8	65.45	62.61	30.7	13.0	0.82	9.15
J1058+5628	0.143	14.0	229.48	219.45	164.4	141.7	3.13	47.88
J1120+4212	0.124	16.9	23.54	24.56	20.3	18.1	7.81	11.69
J1136+6737	0.136	15.3	45.15	-	31.1	16.2	14.8	6.10
J1145-0340	0.167	16.2	18.65	10.48	<0.6	<1.8	4.1	-
J1156+4238	0.172	15.6	15.64	14.38	<0.6	<1.5	0.69	-
J1201-0007	0.165	15.7	69.51	67.57	8.0	5.5	1.05	-
J1201-0011	0.164	16.7	27.98	23.47	<0.9	<2.1	0.56	-
J1215+0732	0.136	14.8	138.81	81.80	45.6	<2.1	3.27	-
J1217+3007	0.130	14.5	587.82	466.45	262.3	217.4	24.9	54.92
J1221+0821	0.132	16.3	178.36	162.53	15.8	8.6	1.14	-
J1221+2813	0.102	14.3	738.97	921.26	337.2	226.2	1.3	55.39
J1221+3010	0.182	15.7	72.01	62.49	29.5	23.4	16.3	28.12
J1231+6414	0.163	14.3	59.31	-	43.5	1.6	2.49	-
J1253+0326	0.066	12.7	107.35	79.21	36.6	25.2	1.67	-
J1257+2412	0.141	15.7	13.07	10.32	<0.6	<0.6	7.22	-
J1341+3959	0.172	14.9	85.63	57.85	<0.9	<0.9	5.15	-
J1419+5423	0.153	13.8	818.16	581.55	959.5	819.7	0.81	7.66
J1427+3908	0.165	18.0	6.96	4.79	<0.6	<3.0	0.16	-
J1427+5409	0.106	11.8	44.76	29.79	13.7	9.5	0.38	-
J1428+4240	0.129	14.4	57.52	42.72	22.5	10.8	35.5	7.54
J1436+5639	0.150	17.6	20.71	17.11	6.5	6.2	1.67	4.74
J1442+1200	0.163	15.2	67.95	69.97	27.4	5.9	7.82	4.55
J1510+3335	0.114	15.1	7.36	4.10	<0.6	<0.6	2.53	-
J1516+2918	0.130	14.6	136.51	73.96	31.6	3.5	1.27	-
J1534+3715	0.143	16.3	20.96	21.57	14.4	<1.2	0.23	4.49
J1604+3345	0.177	18.0	7.09	5.84	<0.6	<0.6	0.72	-
J1647+2909	0.132	13.4	394.72	275.79	56.4	7.0	0.43	-

N.O means that the source is not osberved.